Materialia 6 (2019) 100286

Contents lists available at ScienceDirect

Materialia

journal homepage: www.elsevier.com/locate/mtla

Full Length Article

Hysteretic energy dissipation in aluminium matrix syntactic foam under intermittent cyclic compression

Yue Zhang, Yuyuan Zhao*

School of Engineering, University of Liverpool, Liverpool L69 3GH, UK

ARTICLE INFO

Keywords:
Metal matrix syntactic foam
Cyclic loading
Hysteretic energy dissipation
Specific damping capacity
Damping mechanism

ABSTRACT

Metal matrix syntactic foams with an Al 6082 matrix and hollow SiO_2-Al_2O_3 microspheres were fabricated by infiltration casting. The energy absorption behaviours of the syntactic foams under monotonic, intermittent cyclic and two-stage repetitive cyclic compression conditions were studied. The compressive strength, yield strain and plateau stress are mainly dependent on the CM particle size and are less sensitive to the CM volume percentage. The specific dissipated energy under cyclic loading is mainly dependent on the loading stress and is proportional to the square of stress. Each syntactic foam has a nearly constant hysteretic specific damping capacity, which is proportional to the CM volume percentage but is not sensitive to the CM particle size. The cyclic loading history has an influence on the hysteretic energy dissipation. If the stress level is below the maximum stress experienced in the previous cycles, the specific dissipated energy and specific damping capacity are much lower than those measured at the same stress in previous cycles. The hysteretic energy dissipation is caused by microcrack formation and propagation in the CM particles. The accumulation of crack development leads to CM particle fracture, which results in a small permanent plastic deformation.

1. Introduction

Metal matrix syntactic foam (MMSF) is a special composite material where a metal matrix is embedded with hollow or porous ceramic particles. Using hollow or porous ceramic particles as the reinforcement gives MMSF many outstanding mechanical properties, such as low density, high specific stiffness, high energy absorbing and damping capability [1]. MMSF is a candidate material for several structural components in automobiles and other modes of transportation because they can reduce weight and improve fuel efficiency [2]. Meanwhile, its porous structure provides a capability of a large amount of plastic deformation and thus an energy absorption capacity under compression or impact. It can serve as a protective material by sacrificing itself against damages caused by collision or impact. MMSF also has a good damping capacity so can be used in applications for mitigating vibration [3].

The research to date on the mechanical properties of MMSF has largely been focused on its energy absorbing capacity under compression and impact. Its energy absorption capacity can be evaluated by the area under the compressive stress-strain curve up to the onset of densification where the hollow or porous ceramic particles are fully crushed [4]. MMSF can absorb a huge amount of energy due to extensive strain accumulation at a relatively high plateau stress resulting from the reinforcing ceramic particles and a high densification strain, which is directly determined by the porosity of the MMSF [1,5–16].

Compared to the vast amount of literature available on the compressive properties of MMSF, however, the study on the damping capacity of MMSF is very limited. Wu et al. [3] measured the damping properties of the 6061Al/hollow sphere fly ash syntactic foam with different particle sizes by a multifunctional internal friction apparatus, in both the forced-vibration and bending-vibration modes. Their results showed that the syntactic foams with small particles had higher damping capacities than those with large particles in both vibration modes, and the damping capacity measured in the bending-vibration mode was more than twice of that measured in the forced-vibration mode. Cox et al. [2] and Licitra et al. [17] studied the damping behaviour of A356 matrix syntactic foams reinforced with hollow SiC and alumina particles, respectively, using a dynamic mechanical analyser (DMA) in the three-point bending mode. They found that the damping parameter of the syntactic foam with a lower density was lower than that of the syntactic foam with a higher density and both were lower than that of the A356 alloy, indicating small contributions from the hollow ceramic particles in damping. Katona et al. [18] studied the damping behaviour of Al matrix syntactic foams with Al-Si alloy matrices and hollow Al_2O_3-SiO_2 spheres by DMA and showed that the matrix had a significant effect on the loss factor. In these studies, the dynamic tests were conducted at low stress, low

* Corresponding author.
E-mail address: y.y.zhao@liv.ac.uk (Y. Zhao).

https://doi.org/10.1016/j.mtla.2019.100286
Received 6 February 2019; Accepted 2 March 2019
Available online 08 March 2019

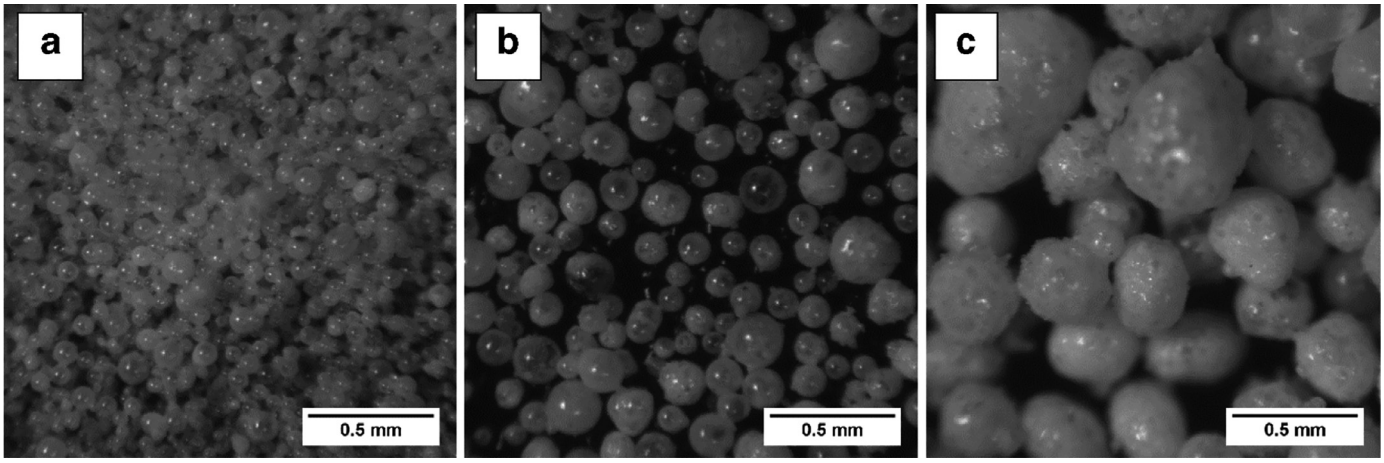

Fig. 1. Morphologies of the ceramic microspheres with particle size ranges of: (a) 75–150 μm (b) 125–250 μm and (c) 250–500 μm.

strain conditions in the elastic region. The investigations were generally confined to the effects of particle size, temperature and test conditions on the damping capacity of a number of MMSFs. The mechanism of energy dissipation in dynamic damping in syntactic foams, especially under high stress conditions, has rarely been investigated.

In this study, MMSFs with an Al 6082 alloy matrix and different sized hollow ceramic microspheres have been manufactured by the melt infiltration casting method. The energy absorption and damping capacity of the syntactic foams have been studied under monotonic, intermittent cyclic and two-stage repetitive cyclic compression conditions. A new energy dissipation mechanism has been proposed to interpret the characteristic damping behaviour of the MMSFs under cyclic compression.

2. Experimental

2.1. Raw materials

The raw materials used to produce the aluminium matrix syntactic foam samples are the commercial 6082 Al alloy and a ceramic microsphere (CM) powder supplied by Envirospheres Pty Ltd. The CM powder is composed of 55–65% SiO_2, 30–36% Al_2O_3, 1–2% Fe_2O_3 and 0.5–1% TiO_2 by weight, and has an effective density (the mass of the powder divided by the volume of the particles, without the air voids between them) of 0.66 g/cm^3. The CM powder was divided into three particle size ranges, 75–150 μm, 125–250 μm and 250–500 μm, as shown in Fig. 1. The wall thickness of the CM particles is approximately 10% of the particle diameter.

2.2. Production process

The Al matrix syntactic foam samples were produced by the melt infiltration casting process as illustrated schematically in Fig. 2. The process consisted of the following steps. (1) An Al block and a CM powder were prepared with a volume ratio of 1:2, with the Al slightly more than the amount needed to ensure full infiltration into the CM powder. (2) The CM powder was filled into a steel tube mould with the bottom sealed by a circular steel disc. The Al block, in the form of a cylinder, was then placed on top of the packed bed of CMs, separated by an ultrathin Kaowool filter paper. The filter paper was used to prevent contact between the Al melt and the CMs before pressure was applied and also to filter aluminium oxide films during infiltration. Another circular steel disc, which was slightly smaller than the internal diameter of the steel tube, was subsequently placed on top of the Al block. (3) The whole assembly was heated up and maintained at 730 °C for 30 min in an electric furnace to fully melt the Al block. (4) The assembly was then moved to a hydraulic press and was rapidly compressed so that the molten Al infiltrated into the interstices between the CM particles. (5) After complete solidification of Al, the syntactic foam sample was removed from the steel tube mould. The steel discs and the extra Al layer at the top of the sample was then removed and the resultant syntactic foam sample was machined and ground to the desired shape and dimensions for subsequent tests. The syntactic foam samples have a nearly constant CM volume percentage of 60%, because a randomly packed spherical powder occupies approximately 60% of the total volume [19].

Three additional sets of samples with lower CM volume percentages were produced following the same procedure, except step (2). For these samples, the CM powder was firstly mixed with an Al 6082 powder, using a small amount of ethanol as binder, before step (3) [20]. The volume ratios between the Al and CM powders were 2:1, 5:7 and 1:5, resulting in CM volume percentages in the syntactic foam samples of 20%, 35% and 50% respectively. The density of the syntactic foam samples was measured by the Archimedes' method using water as the working medium.

2.3. Compression tests

Three types of compression test, namely monotonic, intermittent cyclic and repetitive cyclic, were carried out. The syntactic foam specimens were machined to a cubic form with dimensions $15 \times 15 \times 15$ mm^3 and polished prior to testing. A thin layer of multipurpose grease was applied on the surface of the specimens as a lubricant to avoid the specimen barrelling effect due to friction during compression. All the compression tests were conducted at room temperature on an Instron 4045 test system equipped with a 50 kN load cell, with a strain rate of 10^{-3} s^{-1} to ensure quasi-static compression [21]. The load and displacement data were acquired with Bluehill 2.0 software and processed by Microsoft Excel.

In the monotonic compression tests, the syntactic foam specimens were compressed uniaxially to an engineering strain of 0.7 until the specimen was completely crushed. Three specimens of each type of syntactic foam were tested and the compressive properties were characterised by the average values of the three tests.

In the intermittent cyclic compression tests, the specimens were compressed uniaxially to a strain of 0.01, unloaded and then reloaded to a strain of 0.02. The unloading-loading cycles were repeated 6 more times at different strains up to 0.08 with an interval of 0.01.

The repetitive cyclic compression tests were conducted on one syntactic foam specimen with small CMs (75–150 μm) in two stages. In stage 1, the tests were conducted first at 30 MPa, then at 60 MPa and finally at 80 MPa for 50 unloading-loading cycles each. In stage 2, the same tests were conducted again on the same specimen sequentially at 30 MPa, 60 MPa and 80 MPa, each for 50 unloading-loading cycles. The

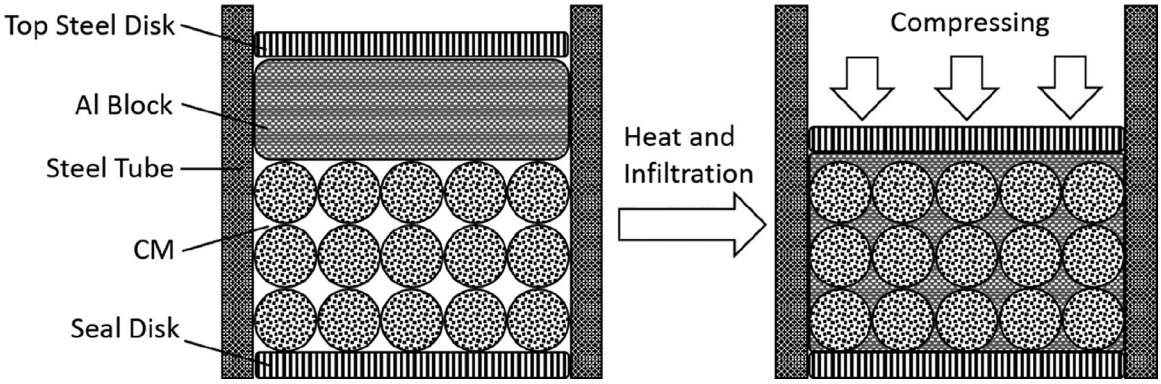

Fig. 2. Schematic of melt infiltration casting process.

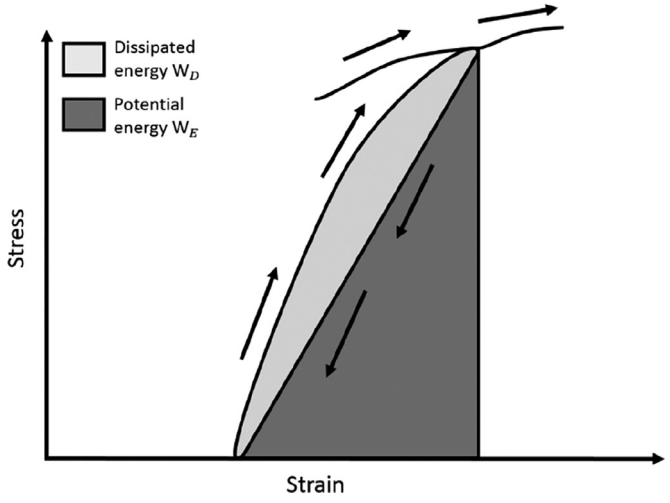

Fig. 3. Schematic diagram of an unloading-loading cycle showing the amounts of dissipated energy and elastic energy.

two stage tests were designed to investigate the difference of energy dissipation between fresh and further repetitive cyclic loading.

Fig. 3 is a schematic diagram of an unloading-loading cycle and the hysteresis loop formed, with the arrows indicating the unloading and reloading sequence. The dissipated energy, or hysteretic energy loss, W_D, corresponds to the area enclosed by this hysteresis loop, while the area under the lower path (unloading part) of the hysteresis curve represents the elastic energy stored, W_E. The specific dissipated and elastic energies were determined by dividing W_D and W_E by the initial volume of the specimen. The specific damping capacity is the ratio of the energy dissipated in a cycle to the elastic or potential energy stored in this cycle [22,23] and was determined by:

$$\psi = \frac{W_D}{W_E} \quad (1)$$

3. Results

3.1. Microstructure and density

The typical microstructures of the Al matrix syntactic foams are shown in Fig. 4. For all the three particle size ranges, the distribution of the CMs in the Al matrix is random and homogeneous, showing that the molten Al has fully infiltrated into the interparticle spaces in the closely packed bed of CMs. An intimate contact between the matrix and the CM particles can be observed (Fig. 4(d)), indicting good wetting at the matrix-CM interface. However, some CM particles (less than 10%) were infiltrated by Al due to their broken structure.

The syntactic foam specimens with three different CM particle sizes but the same CM volume percentage of 60% had similar density values in a narrow range of 1.4–1.45 g/cm^3. When the CM volume percentage was reduced to 50%, 35% and 20%, the density of the syntactic foam increased to 1.70, 1.98 and 2.29 g/cm^3, respectively.

3.2. Monotonic compression

The representative stress-strain curves of the syntactic foams with different CM particle size ranges and different CM volume percentages, under quasi-static compression, are shown in Fig. 5. Similar to the previous observations [1,5–16], the stress-strain curves are characterised by three regions, namely elastic, plateau and densification regions.

The characteristic compressive properties of the syntactic foams under the quasi-static compression, obtained by averaging the values of three specimens, are summarized in Table 1. The compressive strength is defined according to ISO 13,314 as the maximum stress at fracture or collapse of the foam and the plateau stress is the mean of the stress in the plastic deformation region after the initial drop until the densification strain [21]. The yield strain is the strain corresponding to the yield stress. The densification strain is defined as the intersection of the tangents to the plateau region and the densification region [24]. The specific energy absorption, which quantifies the energy absorption capacity of the syntactic foam, is the area under the stress-strain curve up to the densification.

Table 1 shows that compressive strength, yield strain and plateau stress are mainly dependent upon the CM particle size (cf. specimens 1–3). The Al matrix syntactic foams with the smallest CM particles (specimen 1) have the highest compressive stress and plateau stress, while those with the largest CM particles (specimen 3) have the lowest compressive stress and plateau stress. This is because the smaller CM particles produce a stronger strengthening effect, if the spheres being compared have the same wall thickness or the same thickness-to-radius ratio [4]. The yield strain follows the same pattern as the yield stress, because all the specimens have a very similar elastic modulus, as evidenced in Fig. 5.

The compressive strength, yield strain and plateau stress are less sensitive to the CM volume percentage (cf. specimens 4–6). Reducing the CM volume percentage from 50% to 35% and to 20% by increasing the amount of Al particles in the syntactic foam samples has an insignificant effect on the compressive strength, because the strength of syntactic foams is determined by the compressive strength of the CMs rather than the volume fraction of the Al matrix in this case [20]. Compared with the normal syntactic foam samples without Al particle toughening (specimen 2), the compressive strength of the samples toughened with Al particles (specimens 4–6) is improved by 24–36 MPa. This improvement of compressive strength, however, can be attributed to the different failure modes between the normal and Al particle toughened

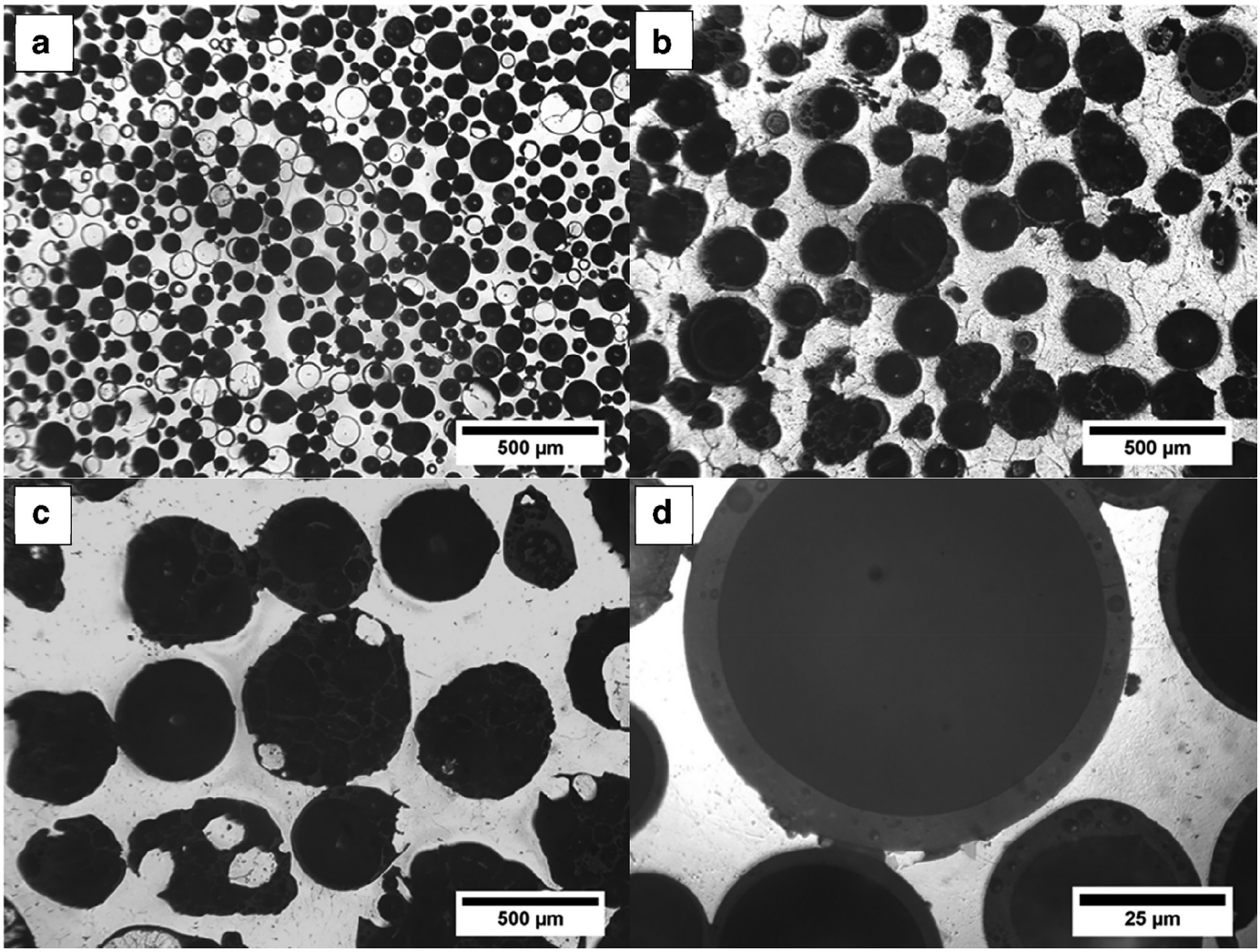

Fig. 4. Optical micrographs of the Al matrix syntactic foams with CM particle ranges of (a) 75–150 μm, (b) 125–250 μm and (c) 250–500 μm, and (d) a high magnification image showing the interface between the matrix and CM particles.

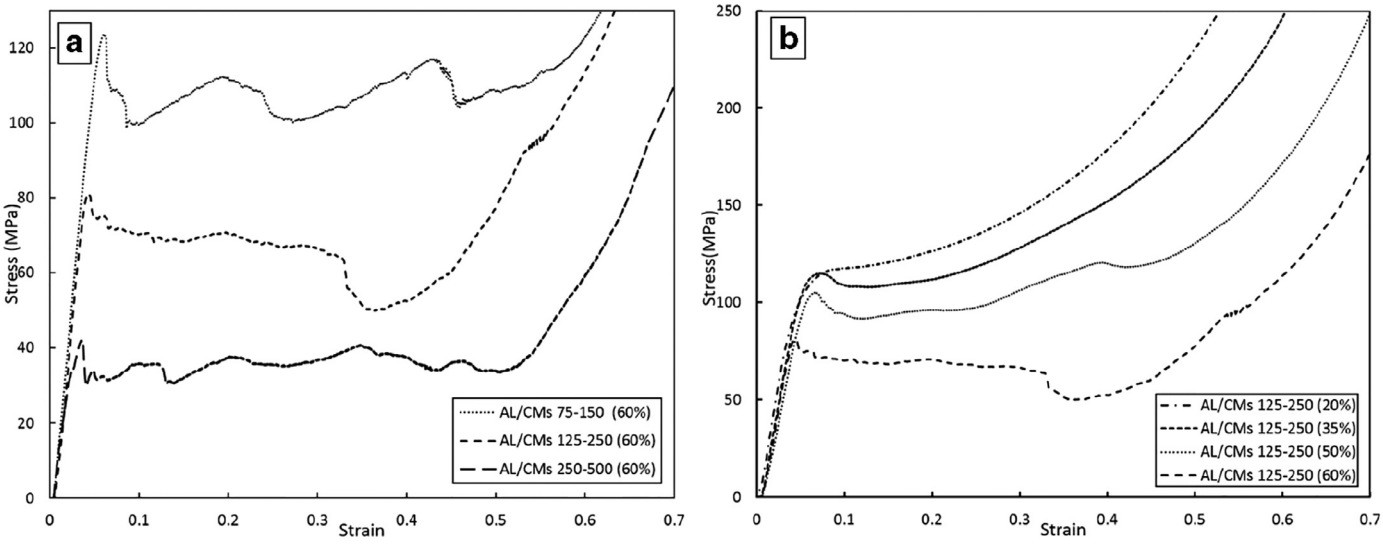

Fig. 5. Representative stress-strain curves of the syntactic foams with different (a) CM particle size ranges and (b) CM volume percentages.

Table 1
Monotonic compressive properties of the Al matrix syntactic foams with different CM particle size ranges and different CM volume percentages.

No.	CM particle size (μm)	CM vol.% (%)	Compressive strength (MPa)	Yield strain	Plateau stress (MPa)	Densification strain	Specific energy absorption (MJ/m^3)
1	75–150	60	123.2 ± 8.5	0.06 ± 0.006	108.5 ± 5.6	0.60 ± 0.05	62.5 ± 2.1
2	125–250	60	80.9 ± 5.1	0.05 ± 0.002	65.3 ± 0.9	0.58 ± 0.02	36.7 ± 0.4
3	250–500	60	41.9 ± 1.1	0.03 ± 0.003	35.7 ± 1.0	0.59 ± 0.01	19.6 ± 0.5
4	125–250	20	116.5 ± 1.7	0.07 ± 0.007	116.0 ± 1.0	0.32 ± 0.06	36.9 ± 0.2
5	125–250	35	115.8 ± 1.5	0.07 ± 0.006	110.7 ± 1.7	0.38 ± 0.06	41.9 ± 0.8
6	125–250	50	105.2 ± 2.0	0.07 ± 0.003	98.4 ± 1.4	0.51 ± 0.07	51.1 ± 0.1

syntactic foams [20]. The normal syntactic foam samples failed by shear or cracking, while the syntactic foam samples toughened with Al particles failed by collapse and crushing of the CMs.

Table 1 also shows that the densification is mainly determined by the CM volume percentage (specimens 2, 4–6). This is not surprising because the upper limit of the densification strain is the total porosity of the syntactic foam, which directly depends on the CM volume percentage. The specific energy absorption is a function of both the plateau stress and the densification strain as expected and can be approximated by their product. The specific energy absorption values of the three types of syntactic foams are in the range of 20–63 MJ/m^3 (specimens 1–3) are considerably higher than those of Al foams, which are usually less than 13 MJ/m^3 [25].

3.3. Intermittent cyclic compression

The typical stress-strain curves of the syntactic foams with different CM particle sizes and different CM volume percentages under intermittent cyclic loading are shown in Fig. 6. Excluding the appreciable hysteresis loops of the unloading-loading cycles at the given strains, the envelop curves broadly coincide with the stress-strain curves of the corresponding syntactic foams under monotonic compression.

Fig. 7 compares the specific dissipated energy at different strains for the syntactic foams with different CM particle sizes (Fig. 7a) and different CM volume percentages (Fig. 7b). The specific dissipated energy for each unloading-loading cycle is mainly dependent on the stress at which the cyclic loading was conducted, which increased with the strain in the elastic region and fluctuated in the plateau region, depending on whether the deformation was ductile or brittle.

Fig. 7 also compares the specific damping capacity at different strains for the syntactic foams with different CM particle sizes (Fig. 7c) and different CM volume percentages (Fig. 7d). In the first unloading-loading cycle, i.e. at the strain of 0.01, the specific damping capacity was small. A reasonable explanation for the low ratio of the dissipated energy to the stored elastic energy is that the low amplitude of stress in this cycle was high enough to close the voids in the matrix of the syntactic foam, usually present at the Al-CM interfaces, but insufficient to cause significant damages to the CM particles, which is considered to be the key contributor to energy dissipation as will be discussed in Section 4.2. In the subsequent unloading-loading cycles, i.e. at the strains between 0.02 and 0.08, however, the specific damping capacity remained nearly constant for any particular syntactic foam. In other words, the energy dissipated in an unloading-loading cycle was proportional to the elastic or potential energy stored in this cycle, i.e., a fixed proportion of the total energy absorbed by the material was dissipated, regardless of the stress and strain at which the loading cycle was conducted.

Fig. 8 shows that the average specific damping capacity between the strains of 0.02 to 0.08 for each type of syntactic foam is proportional to the CM volume percentage, indicating that the energy dissipation in cyclic loading is due to changes inside the CM particles. The syntactic foams with the same CM volume percentage of 60% but different CM particle sizes show similar specific damping capacity values (0.083–0.088), indicating low sensitivity to CM particle size.

3.4. Repetitive cyclic compression

The stress-strain responses of the syntactic foam specimen reinforced with the small CMs (75–150 μm) under the repetitive cyclic compression in both stage 1 and stage 2 are shown in Fig. 9. To amplify and compare the evolution of the hysteresis loops during cyclic loading in both stages, the 1st, 25th and 50th hysteresis cycles at each stress amplitude for both stage 1 and stage 2 loading are shown side by side in Fig. 10.

Figs. 9 and 10 show that the behaviours of the hysteresis loops generated by the repetitive cyclic compression in the stage 1 and stage 2 are significantly different, in spite of the same loading conditions. In stage 1, the strain displacements and the hysteresis loops are evident at all the three stress amplitudes of 30, 60 and 80 MPa. In stage 2, however, large hysteresis loops are only seen at the highest stress amplitude of 80 MPa. Appreciable hysteresis loops are also exhibited at the intermediate stress amplitude of 60 MPa, but they are narrower than those in stage 1. The hysteresis loops at the lowest stress amplitude of 30 MPa in stage 2 are very small, with nearly overlapping unloading and loading paths.

The evolutions of the hysteresis loops in the two stages are demonstrated more clearly in terms of specific dissipated energy (Fig. 11a) and specific damping capacity (Fig. 11b). As a general observation, the specific dissipated energy tends to decrease with increasing number of cycles in stage 1 but remains unchanged in stage 2. In stage 1, the average magnitudes of the specific dissipated energy at the stress amplitudes of 30, 60 and 80 MPa are approximately 10, 30 and 50 kJ/m^3, respectively. They are similar to those observed in the intermittent cyclic compression. In stage 2, the average magnitudes of the specific dissipated energy at 30 and 60 MPa are reduced considerably to approximately 1 and 13 kJ/m^3, which are approximately 10% and 30% of the stage 1 values, respectively. The specific dissipated energy at 80 MPa in stage 2 follows the same trend as in stage 1, with a slightly lower average magnitude of 45 kJ/m^3.

The difference in energy dissipation behaviour between stage 1 and stage 2 is more visible in terms of the specific damping capacity (Fig. 11 Evolutions of (a) specific dissipated energy). The specific damping capacity is not sensitive to the stress amplitude in stage 1. It varies in a relatively narrow range of 0.06–0.1. In stage 2, however, the specific damping capacity is very sensitive to the stress amplitude and has representative values of 0.005, 0.036 and 0.075 at e stress amplitudes of 30, 60 and 80 MPa, respectively.

The two-stage test results above demonstrate that the cyclic loading history has a direct influence on the hysteretic energy dissipation, depending on whether the stress amplitude is below, equal to or above the maximum stress the specimen has experienced previously. When the stress is above the previous stress levels experienced by the specimen (as shown in stage 1), the previous loading history has very little effect on the hysteretic energy dissipation; the specific dissipated energy and specific damping capacity are solely determined by the current stress amplitude. When the stress is equal to the maximum stress level experienced in the previous cycles (as shown in the case of 80 MPa in stage 2 vs stage 1), the current cyclic loading behaves as a continuation of the previous cyclic loading; the specific dissipated energy and specific damping capacity remain the same in both stages. When the stress is below the maximum stress level experienced in the previous cycles (as shown in

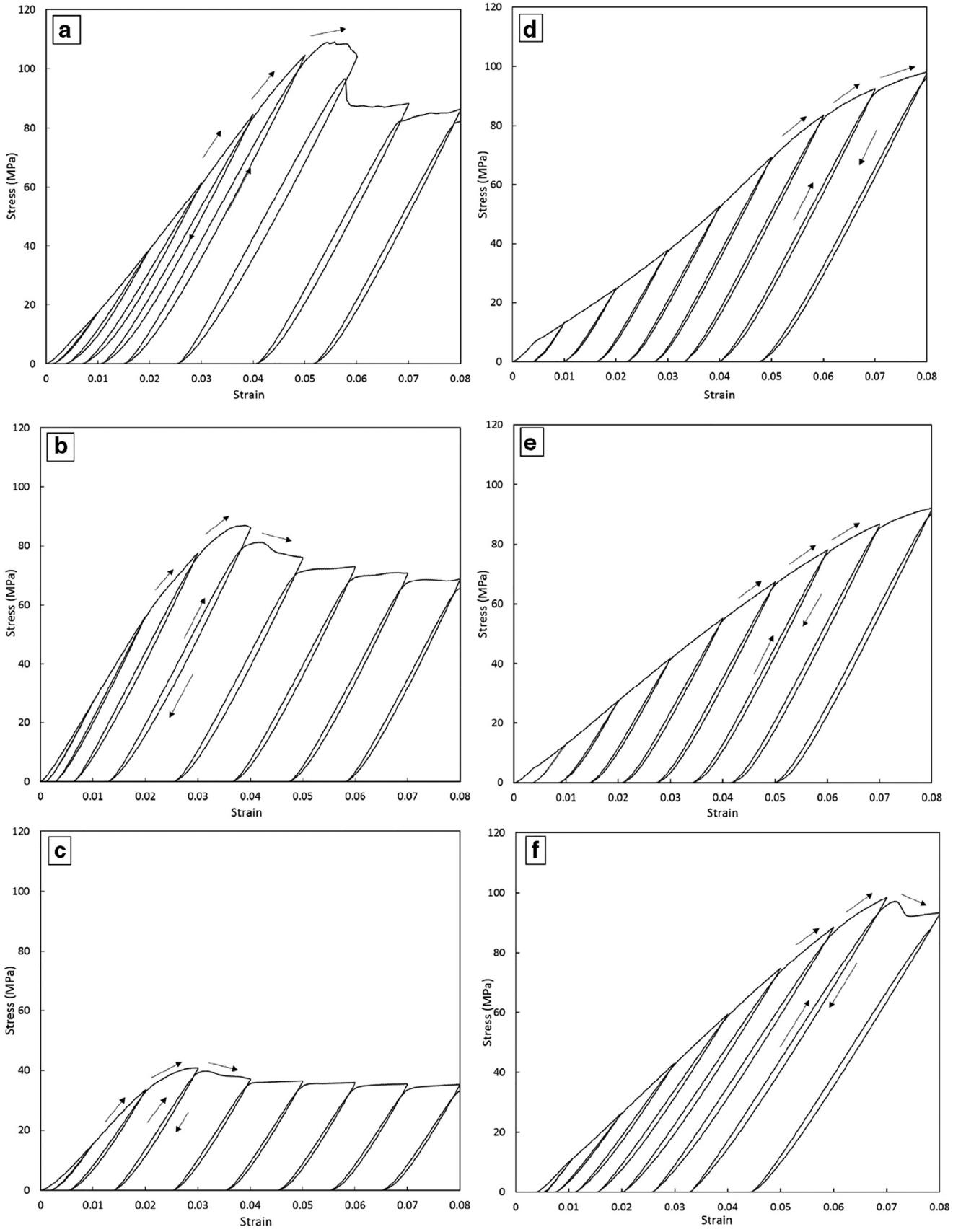

Fig. 6. Typical stress-strain curves of the Al matrix syntactic foams with different CM particle sizes and volume fractions: (a) 75–150 μm, 60%; (b) 125–250 μm, 60%; (c) 250–500 μm, 60%; (d) 125–250 μm, 20%; (e) 125–250 μm, 35%; and (f) 125–250 μm, 50%; under cyclic compression.

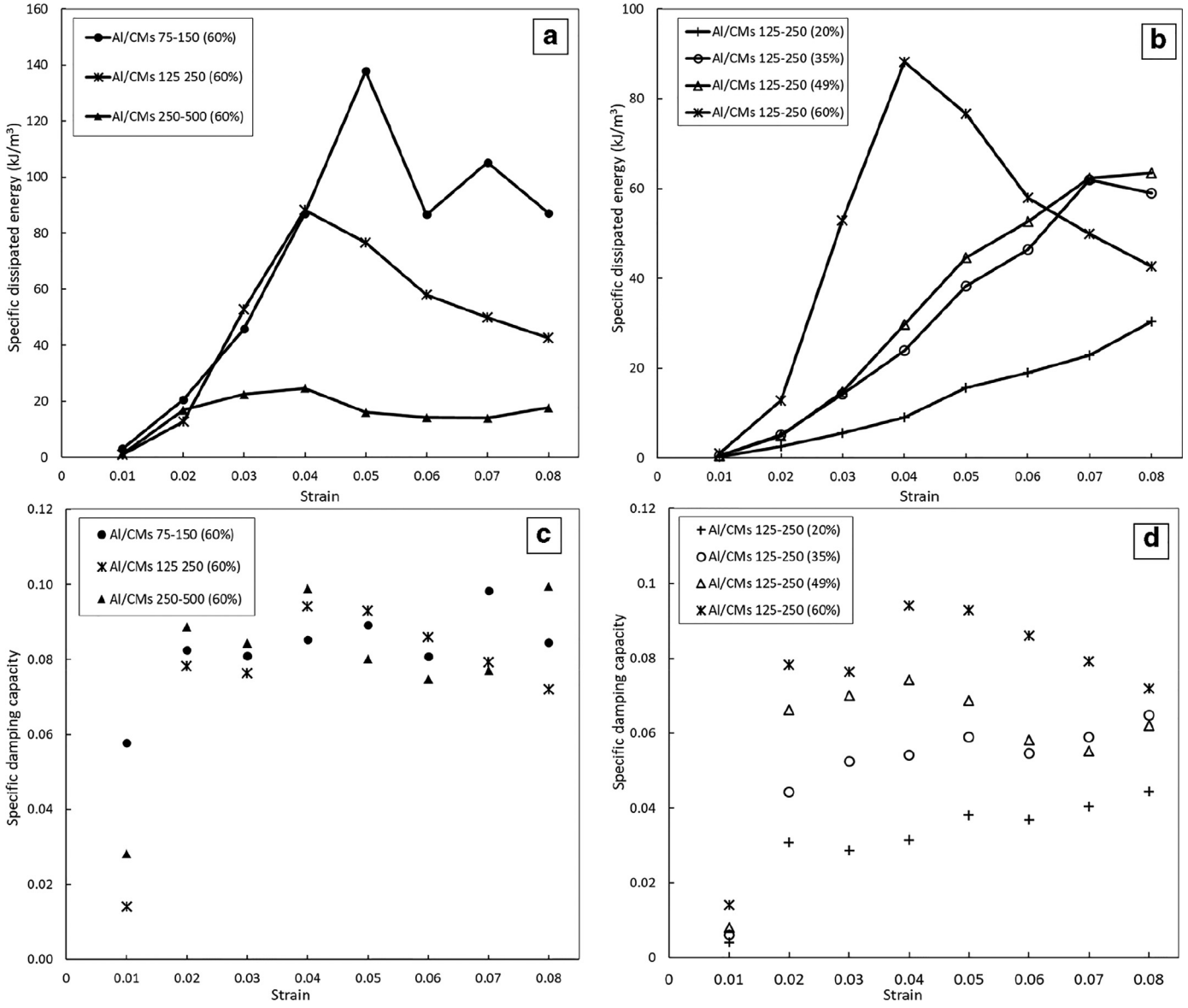

Fig. 7. Hysteretic dissipated energy (a, b) and specific damping capacity (c, d) of each unloading-loading cycle of the syntactic foams with different CM particle sizes (a, c) and different CM volume percentages (b, d).

the cases of 30 MPa and 60 MPa in stage 2), the previous loading history has a strong effect on the hysteretic energy dissipation; the specific dissipated energy and specific damping capacity become much lower than the previous stage; the lower the stress, the greater the reduction in the hysteretic energy dissipation.

4. Discussion

4.1. Specific damping capacity

The specific damping capacity in cyclic loading describes the hysteretic energy dissipation relative to the elastic energy involved in the loading cycle. This elastic energy is the amount of recoverable energy in the unloading-loading cycle and can be expressed by:

$$W_E = \frac{1}{2}\sigma\Delta\varepsilon = \frac{\sigma^2}{2E} \quad (2)$$

where σ is the stress at which the unloading-loading cycle is conducted and $\Delta\varepsilon$ is the elastic strain produced in the cycle, which is approximately equal to the stress divided by the elastic modulus of the syntactic foam, E. As all the syntactic foam specimens have nearly the same elastic modulus (see Fig. 5), the elastic energy involved in cyclic loading is solely determined by the stress of the cyclic loading.

The specific damping capacity of any particular syntactic foam measured at strains between 0.02 and 0.08 does not vary much (Fig. 7). It means that the ratio between the dissipated energy by hysteresis loss, W_D, and the elastic energy involved in the loading cycle, W_E, is nearly a constant. Like the elastic energy, the dissipated energy at strains between 0.02 and 0.07 is also proportional to the square of the applied stress of the cyclic loading, σ^2.

However, the specific damping capacity of the first hysteresis loop measured at the strain of 0.01 in the intermittent cyclic compression is considerably lower than those of the subsequent hysteresis loops (Fig. 7). It is appreciated that the first compression cycle was conducted at a relatively low stress. It seems that this low stress amplitude is not sufficient to initiate the main energy dissipation or damping mechanism prevalent at higher stress amplitudes in the subsequent hysteresis loops.

It is worth noting that the specific damping capacity is one of several parameters that are used to quantify the damping property of

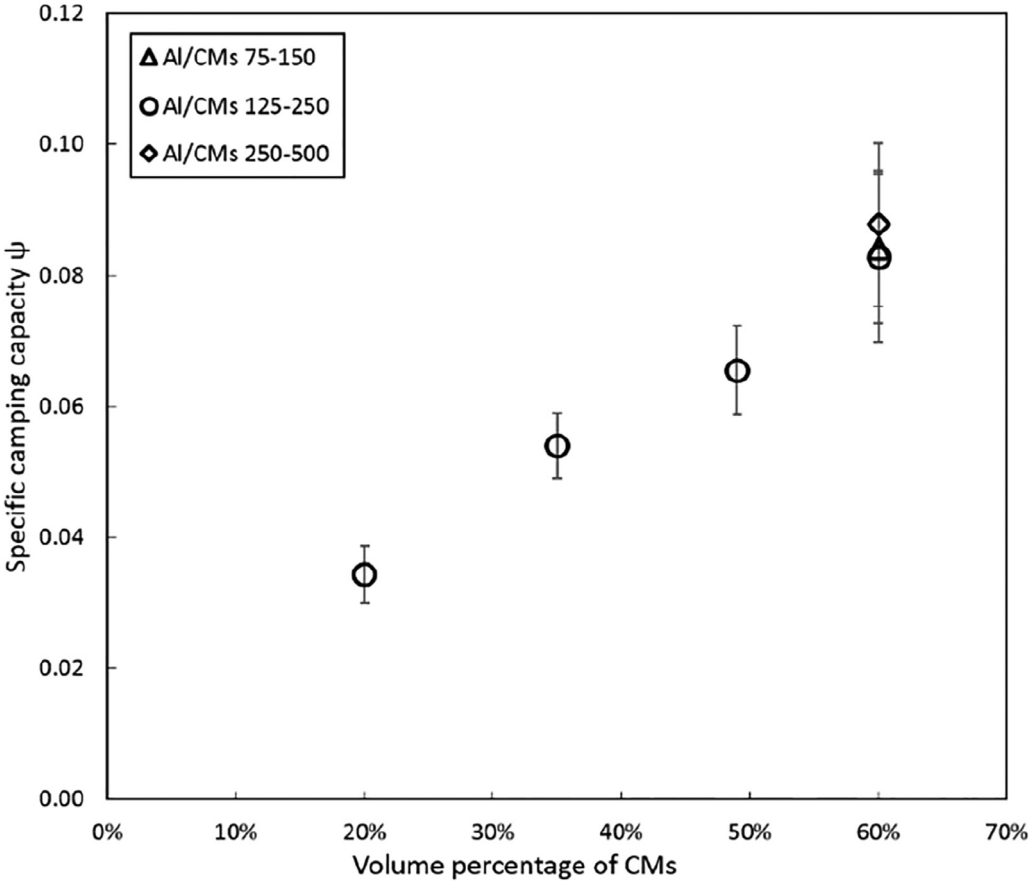

Fig. 8. Specific damping capacity vs CM volume percentage for the syntactic foams.

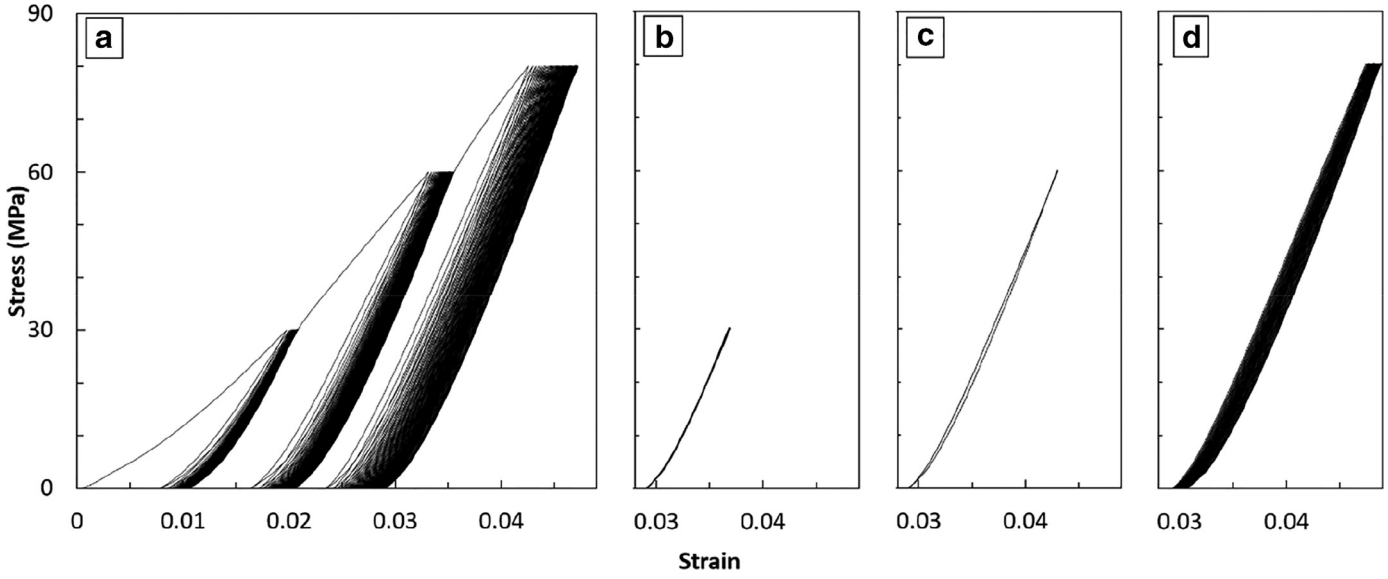

Fig. 9. Stress-strain curves of the syntactic foam under repetitive cyclic compression in (a) stage 1, and stage 2 at (b) 30 MPa, (c) 60 MPa and (d) 80 MPa.

a material. Depending on the measurement methods (such as torsion pendulum, suspended beam, dynamic mechanical thermal analyser, piezoelectric ultrasonic vibration, decay and resonant vibration), a variety of parameters, including loss angle (φ), loss tangent ($\tan\varphi$), inverse quality factor (Q^{-1}), loss factor (η), logarithmic decrement (δ) and specific damping capacity (ψ), are used to characterise the damping capacity. Although these parameters are sensitive to frequency and temperature, they are interchangeable with a proper conversion in cases of relatively small damping capacity ($\tan\varphi < 0.1$) by the following equation [26]:

$$\varphi \approx \tan\varphi = Q^{-1} = \eta = \frac{\Psi}{2\pi} \approx \frac{\delta}{\pi} \tag{3}$$

The order of magnitude of the damping capacity measured in this study is comparable to those measured by Cox et al. [2], Licitra et al. [17] and Katona et al. [18] on Al matrix syntactic foams reinforced with hollow Al_2O_3, SiC or Al_2O_3-SiO_2 particles using dynamic mechanical analyser.

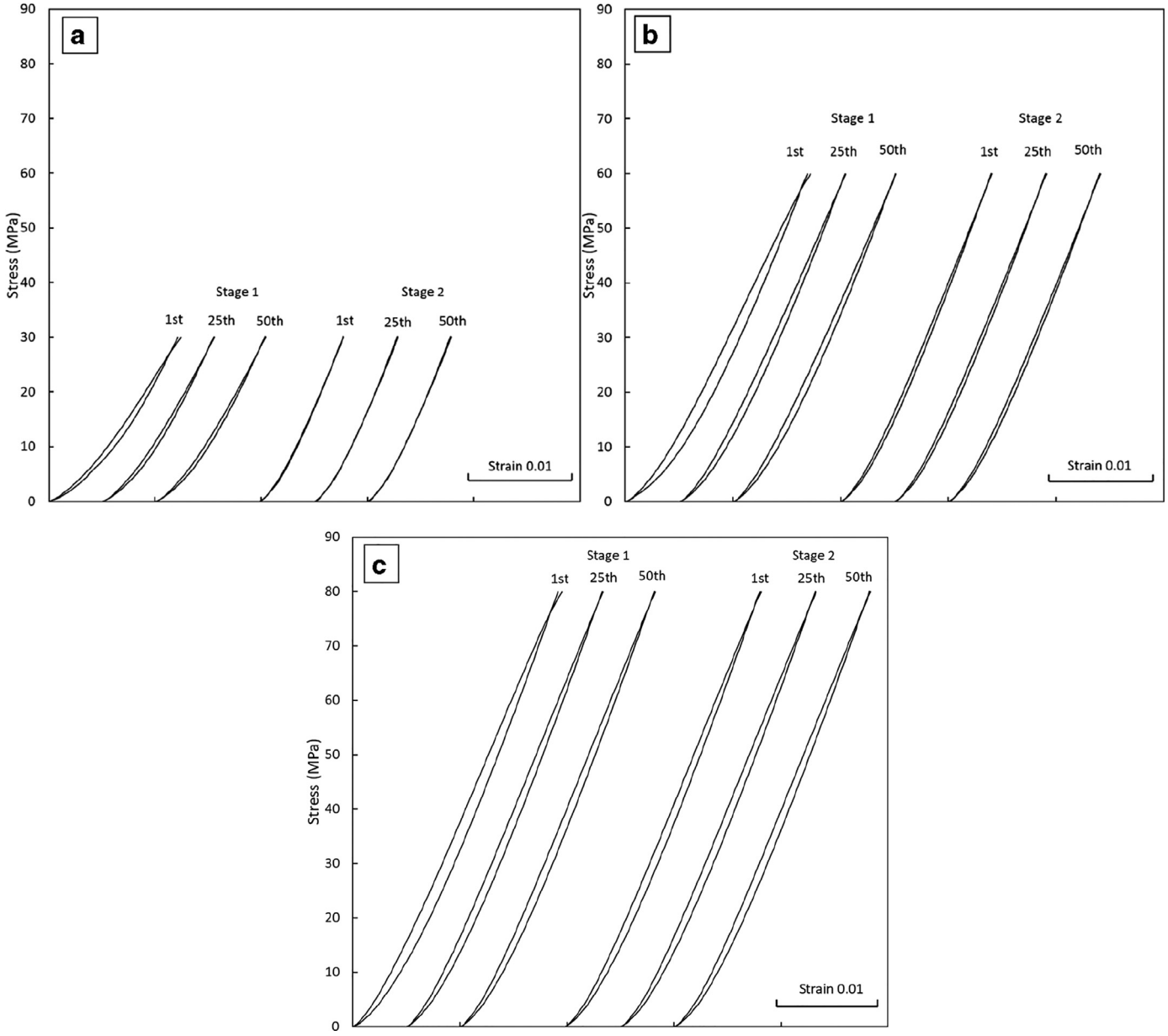

Fig. 10. Hysteresis loops of the 1st, 25th and 50th cycles in the repetitive cyclic compression in stage 1 and stage 2, conducted at (a) 30 MPa, (b) 60 MPa and (c) 80 MPa.

4.2. Damping mechanism

Fig. 8 shows that the specific damping capacity is proportional to the CM volume percentage in the syntactic foam. For the syntactic foams with the same CM volume percentage, CM particle size has little effect on the specific damping capacity (Fig. 7c). It demonstrates that the energy dissipation in cyclic loading mainly occurs inside the CM particles such that the amount of the dissipated energy is directly correlated to the volume percentage of the CM particles in the syntactic foam. The interface between the CM particles and the matrix, which varies with the CM particle size, does not seem to play a part in the energy dissipation.

The stage 1 repetitive cyclic compression of the syntactic foam (Fig. 9a) shows that there is a permanent plastic deformation after each unloading-loading cycle and the amount of the plastic deformation is dependent on the stress at which the cyclic loading is conducted. The accumulative plastic strains after 50 cycles at the applied stresses of 30, 60 and 80 MPa are 0.0011, 0.0024 and 0.0047, which correspond to plastic-deformation-caused energy absorptions of 33, 144 and 376 kJ/m^3 respectively. For each unloading-loading cycle, the average energy absorptions due to plastic deformation are 0.66, 2.88 and 7.52 kJ/m^3 respectively. In comparison, the average hysteretic energy dissipations at the stresses of 30, 60 and 80 MPa are 10, 30 and 50 kJ/m^3, respectively (Fig. 11). Conversely, the hysteretic energy dissipations are approximately 15, 10 and 7 times of the plastic-deformation-caused energy absorptions, for the stresses of 30, 60 and 80 MPa, respectively.

Five observations on the hysteretic energy dissipation can be made from the above analyses:

(1) The main contributor to the hysteretic energy dissipation is the CM particles.
(2) The hysteretic energy dissipation is not due to permanent plastic deformation.
(3) The process generating the hysteretic energy dissipation may contribute to the permanent plastic deformation.
(4) The hysteretic energy dissipation is approximately proportional to the stress squared.

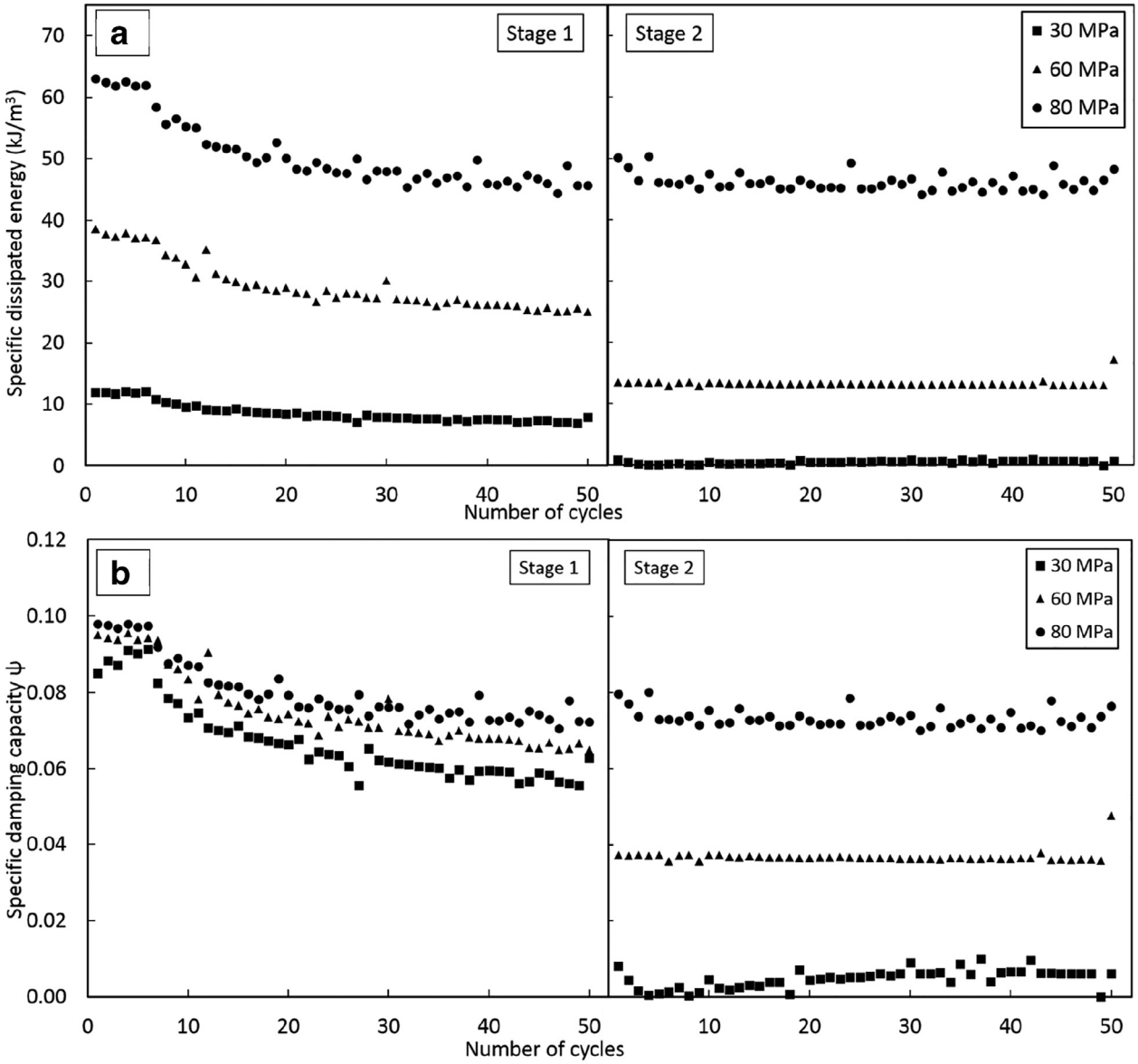

Fig. 11. Evolutions of (a) specific dissipated energy and (b) specific damping capacity in repetitive cyclic compression at different stress amplitudes in stage 1 (left) and stage 2 (right).

(5) A higher stress results in a lower ratio between the hysteretic energy dissipation and the plastic-deformation-caused energy dissipation.

These observations indicate that the energy dissipation is caused by microcrack formation and propagation in the CM particles. Many microcracks have indeed been detected on CMs in the synaptic foam samples after repetitive cyclic loading (Fig. 12). Cox et al. [2] also observed cracks in the hollow SiC particles in an Al matrix syntactic foam after DMA test. According to the Griffith theory of brittle fracture, the critical stress required for crack propagation in a brittle material is proportional to the square root of the specific surface energy of the material, or the energy required to create the crack surfaces is proportional to the square of the applied stress, provided it is above the critical stress [27]. The fact that the dissipated energy by hysteresis loss at strains between 0.02 and 0.08 is proportional to the square of the applied stress ($W_D \propto \sigma^2$) conforms to the Griffith theory. This provides a strong supporting evidence that the key mechanism of hysteretic energy dissipation is microcrack formation and propagation in the CM particles.

The microcrack formation and propagation in the CM particles during the cyclic loading can be described as follows. The metal matrix syntactic foam is essentially a cluster of inherently brittle CM particles interspersed with a metal matrix. As a characteristic of the infiltration casting process adopted in this work, most CM particles are in direct contact with their neighbouring CM particles. Stress concentrations will occur at these contact points and the local stress can be significantly higher than the global stress. When the global stress is above a certain level, say a third of the yield stress of the syntactic foam, the local stresses at some locations will reach the critical stress required for crack initiation and propagation in the CM particles. A higher global stress leads to more stress concentration and in turn more crack initiation and propagation. The energy absorbed in creating the crack surfaces is expected to be proportional to the square of stress, according to the Griffith theory. Once a microcrack develops across a CM particle during repetitive loading, fracture occurs and a small plastic deformation is formed. The permanent plastic deformation and the hysteretic energy absorption are the accumulative effects of formation and propagation of all the microcracks inside CM particles. They are dependent on the local stress at

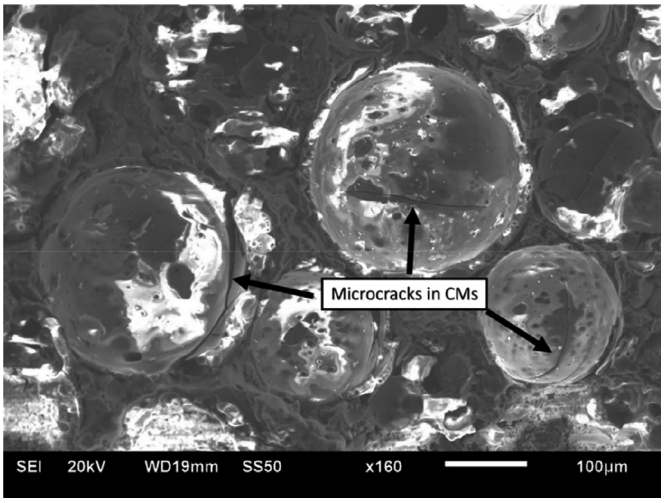

Fig. 12. Scanning electron micrograph of an Al matrix syntactic foam with 250–500 μm CMs after cyclic compression.

the contact points between the CM particles, which in turn is dependent on the stress applied to the syntactic foam sample.

The different hysteretic energy dissipation behaviour in stage 2 from stage 1 cyclic loading at the low and intermediate stress levels can be well explained by the microcrack formation and propagation mechanism. After cyclic loading at 80 MPa for 50 cycles in stage 1, many stress concentration locations that can be activated at a stress below 80 MPa for microcrack propagation have disappeared due to localised plastic deformation. The numbers of microcracks that can form and propagate at stresses of 30 and 60 MPa are reduced, especially significantly at the lower stress. Only when the stress is equal to or above the maximum stress experienced in stage 1, more locations of stress concentration can be activated to form more microcracks and the new and existing microcracks can continue to propagate.

5. Conclusion

(1) In monotonic compression, the compressive strength, yield strain and plateau stress are mainly dependent on the CM particle size and are less sensitive to the CM volume percentage. The densification strain is mainly determined by the CM volume percentage.
(2) In intermittent cyclic compression, the specific dissipated energy in each cycle is mainly dependent on the loading stress and is proportional to the square of stress. For a given syntactic foam, the specific damping capacity is nearly constant, regardless of the stress and strain at which the cyclic loading is conducted, apart from the first loading cycle. The specific damping capacity is proportional to the CM volume percentage, but has low sensitivity to CM particle size.
(3) In repetitive cyclic compression, if the stress level is equal to or above the previous stress amplitudes, the prior loading history has little influence on the hysteretic energy dissipation. If the stress level is below the maximum stress experienced in the previous cycles, the prior loading history has a significant influence on the hysteretic energy dissipation behaviour. The specific dissipated energy and specific damping capacity are much lower than those measured at the same stress in previous cyclic loading.
(4) The hysteretic energy dissipation in the syntactic foam is mainly caused by microcrack formation and propagation in the CM particles. The accumulation of crack development leads to CM particle fracture, which results in a small permanent plastic deformation.

Conflict of interest

The authors have no affiliation with any organization with a direct or indirect financial interest in the subject matter discussed in the manuscript.

Supplementary materials

Supplementary material associated with this article can be found, in the online version, at doi:10.1016/j.mtla.2019.100286.

References

[1] Balcha Dorian K., J.G. O.D., Graham R. Davisc, Carl M. Cady, George T. Gray, David C. Dunanda, Plasticity and damage in aluminum syntactic foams deformed under dynamic and quasi-static conditions, Mater. Sci. Eng. A 391 (1–2) (2005) 408–417.
[2] J. Cox, et al., Dynamic and thermal properties of aluminum alloy a356/silicon carbide hollow particle syntactic foams, Metals 4 (4) (2014) 530–548.
[3] G.H. Wu, et al., Damping properties of aluminum matrix–fly ash composites, Mater. Lett. 60 (24) (2006) 2945–2948.
[4] B. Zhang, et al., Quasi-static and high strain rates compressive behavior of aluminum matrix syntactic foams, Compos. Part B Eng. 98 (Supplement C) (2016) 288–296.
[5] M.D. Goel, et al., Dynamic compression behavior of cenosphere aluminum alloy syntactic foam, Mater. Des. 42 (2012) 418–423.
[6] X. Tao, L. Zhang, Y. Zhao, Al matrix syntactic foam fabricated with bimodal ceramic microspheres, Mater. Des. 30 (7) (2009) 2732–2736.
[7] J.A. Santa Maria, et al., Effect of hollow sphere size and size distribution on the quasi-static and high strain rate compressive properties of Al-A380–Al2O3 syntactic foams, J. Mater. Sci. 49 (3) (2013) 1267–1278.
[8] Y.Y. Zhao, X.F. Tao, Behaviour of metal matrix syntactic foams in compression, in: Proceedings of Materials Science and Technology 2009, Pittsburgh, USA, The Printing House, Stoughton, W1 53589, USA, 2009, pp. 1785–1794.
[9] Q. Zhang, et al., Micro-CT characterization of structural features and deformation behavior of fly ash/aluminum syntactic foam, Acta Mater. 57 (10) (2009) 3003–3011.
[10] D. Lehmhus, et al., Quasi-static and Dynamic Mechanical Performance of Glass Microsphere- and Cenosphere-based 316L Syntactic Foams, Proc. Mater. Sci. 4 (2014) 383–387.
[11] A. Szlancsik, et al., Compressive behaviour of aluminium matrix syntactic foams reinforced by iron hollow spheres, Mater. Des. 83 (2015) 230–237.
[12] G. Castro, S.R. Nutt, X. Wenchen, Compression and low-velocity impact behavior of aluminum syntactic foam, Mater. Sci. Eng. A 578 (Supplement C) (2013) 222–229.
[13] K. Májlinger, I.N. Orbulov, Characteristic compressive properties of hybrid metal matrix syntactic foams, Mater. Sci. Eng. A 606 (2014) 248–256.
[14] I.N. Orbulov, J. Ginsztler, Compressive characteristics of metal matrix syntactic foams, Compos. Part A Appl. Sci. Manuf. 43 (4) (2012) 553–561.
[15] X.F. Tao, Y.Y. Zhao, Compressive failure of Al alloy matrix syntactic foams manufactured by melt infiltration, Mater. Sci. Eng. A 549 (2012) 228–232.
[16] N. Gupta, W. Ricci, Comparison of compressive properties of layered syntactic foams having gradient in microballoon volume fraction and wall thickness, Mater. Sci. Eng. A 427 (1–2) (2006) 331–342.
[17] L. Licitra, et al., Dynamic properties of alumina hollow particle filled aluminum alloy A356 matrix syntactic foams, Mater. Des. 66 (2015) 504–515.
[18] B. Katona, et al., Compressive characteristics and low frequency damping of aluminium matrix syntactic foams, Mater. Sci. Eng. A 739 (2019) 140–148.
[19] M. Hartmann, et al., Microstructure and mechanical properties of cellular magnesium matrix composites, in: Proceedings of the International Conference on Metal Foams and Porous Metal Structures, 1999.
[20] X. Tao, Y. Zhao, Compressive behavior of Al matrix syntactic foams toughened with Al particles, Scr. Mater. 61 (5) (2009) 461–464.
[21] (ISO), I.O.f.S., Mechanical Testing of Metals-Ductility Testing-Compression Test for Porous and Cellular Metals, ISO, Genva, Switzerland, 2011.
[22] S. Liu, et al., Cyclic compression behavior and energy dissipation of aluminum foam–polyurethane interpenetrating phase composites, Compos. Part A Appl. Sci. Manuf. 78 (2015) 35–41.
[23] J. Zhang, R.J. Perez, E.J. Lavernia, Documentation of damping capacity of metallic, ceramic and metal-matrix composite materials, J. Mater. Sci. 28 (9) (1993) 2395–2404.
[24] T.G. Nieh, K. Higashi, J. Wadsworth, Effect of cell morphology on the compressive properties of open-cell aluminum foams, Mater. Sci. Eng. A 283 (1) (2000) 105–110.
[25] M. Kiser, M.Y. He, F.W. Zok, The mechanical response of ceramic microballoon reinforced aluminum matrix composites under compressive loading, Acta Mater. 47 (9) (1999) 2685–2694.
[26] H. Lu, et al., Design, Fabrication, and Properties of High Damping Metal Matrix Composites—A Review, Materials 2 (3) (2009) 958.
[27] B. Lawn, Fracture of Brittle Solids, 2 ed, Cambridge University Press, Cambridge, 1993 Cambridge Solid State Science Series.